sustainability

MDPI

Article

Studies on the Utilization of Marble Dust, Bagasse Ash, and Paddy Straw Wastes to Improve the Mechanical Characteristics of Unfired Soil Blocks

Tarun Sharma [1], Sandeep Singh [2], Shubham Sharma [3,4,*], Aman Sharma [5], Anand Kumar Shukla [6], Changhe Li [4], Yanbin Zhang [4] and Elsayed Mohamed Tag Eldin [7,*]

1 Department of Civil Engineering, Chandigarh University, Mohali 140413, India
2 Department of Civil Engineering, University Center for Research and Development, Chandigarh University, Mohali 140413, India
3 Mechanical Engineering Department, University Center for Research and Development, Chandigarh University, Mohali 140413, India
4 School of Mechanical and Automotive Engineering, Qingdao University of Technology, Qingdao 266520, China
5 Department of Mechanical Engineering, GLA University, Mathura 281406, India
6 Chandigarh School of Business, Chandigarh Group of Colleges, Jhanjheri, Mohali 140308, India
7 Faculty of Engineering and Technology, Future University in Egypt, New Cairo 11835, Egypt
* Correspondence: shubham543sharma@gmail.com or shubhamsharmacsirclri@gmail.com (S.S.); elsayed.tageldin@fue.edu.eg (E.M.T.E.)

Abstract: Earthen materials are the world's oldest and cheapest construction materials. Compacted soil stabilised blocks are unfired admixed soil blocks made up of soil plus stabilisers such as binders, fibres, or a combination of both. The manufacturing and usage of cement and cement blocks raises a number of environmental and economic challenges. As a result, researchers are attempting to develop an alternative to cement blocks, and various tests on unfired admixed soil blocks have been performed. This investigation undertakes use of agricultural waste (i.e., paddy straw fiber and sugarcane bagasse ash) and industrial waste (i.e., marble dust) in manufacturing unfired admixed soil blocks. The applicability of unfired soil blocks admixed with marble dust, paddy straw fiber, and bagasse ash were studied. The marble dust level ranged from 25% to 35%, the bagasse ash content ranged from 7.5% to 12.5%, and the content of paddy straw fibre ranged from 0.8% to 1.2% by soil dry weight. Various tests were conducted on 81 mix designs of the prepared unfired admixed soil blocks to determine the mechanical properties of the blocks, followed by modeling and optimization. The characterization of the materials using XRD and XRF and of the specimens using SEM and EDS were performed for the mineral constituents and microstructural analysis. The findings demonstrate that the suggested method is a superior alternative to burned bricks for improving the mechanical properties of unfired admixed soil blocks.

Keywords: tensile strength; flexural strength; paddy straw; marble dust; soil block

check for updates

Citation: Sharma, T.; Singh, S.; Sharma, S.; Sharma, A.; Shukla, A.K.; Li, C.; Zhang, Y.; Eldin, E.M.T. Studies on the Utilization of Marble Dust, Bagasse Ash, and Paddy Straw Wastes to Improve the Mechanical Characteristics of Unfired Soil Blocks. *Sustainability* **2022**, *14*, 14522. https://doi.org/10.3390/su142114522

Academic Editors: Ivana Barišić and Ivanka Netinger Grubeša

Received: 2 September 2022
Accepted: 24 October 2022
Published: 4 November 2022

1. Introduction

Unfired admixed adobe blocks can be utilized in a number of civil engineering applications, including wall construction blocks, interlocking pavement tiles, and other structures [1,2]. Compacted stabilised adobe blocks are construction units made by adding the right amount of water to the right kind of soil to achieve maximum density and compressing with a block-forming machine. [3] Hand-operated or mechanically operated block making equipment is available. Compared to burnt earth bricks, this represents a more environmentally friendly approach to making compacted stabilised soil blocks. Compacted soil stabilised blocks differ from fired earth bricks in that they do not require the use of a brick kiln, which produces a lot of pollution. The construction industry has already discovered a higher performing equivalent for burnt clay bricks, namely, fly ash blocks and cement blocks, which are commonly employed in the construction of structures [4]. However, the manufacturing and usage of cement and cement blocks raises a number of environmental and economic challenges. As a result, researchers are attempting to develop alternatives to cement blocks, and various tests on unfired admixed soil blocks have been carried out. Different binders and fibers are used for the manufacturing of unfired admixed soil block [5–8]. Bitumen emulsion, cement, grit [9], sugarcane bagasse ash, limestone waste, lime, calcium silicate [10], limestone residues [11], granite waste, demolition residue [12], kaolin, rice husk ash, *Bacillus pasteurii* KCTC 3558 [13], construction debris, fly ash, green mussel shell powder [1], and effective microorganisms (EM) are among the binders used. Natural and synthetic fibres have been employed in various studies, with coconut fibre being the most commonly used. Solid blocks and hollow blocks were used in the bulk of the experiments, with cubic and cylindrical samples studied as well [11–13]. The soil–binder–fiber mixture is deposited in the press chamber for block production, eliminating voids while increasing density. As indicated in previous studies, investigations found a contribution to tensile strength using only fibres. However, in circumstances when both binders and fibres were utilised, tensile strength could be increased further. A typical trend of increasing tensile strength of the compacted admixed adobe blocks with the addition of fibres has been observed, as fibres aid in providing an interlock between soil, binders, and fibres [3,7]. Jute fibre has been shown to have the highest improvement in tensile strength (409%), followed by banana fibre (291%) and polypropylene fibre (179%). A soil admixed block's flexural strength indicates the maximum stress it has been subjected to immediately before yielding. The addition of binders and fibres causes a general improvement in flexural strength, as fibres aid in providing an interlock [14] between soil and fibres or soil, binder, and fibres, resulting in a harder matrix with increased flexural strength. However, studies on the mechanical aspects of compacted soil blocks admixed with paddy straw fibre (PSF), marble dust (MD), and bagasse ash (BA) and its computational analysis were not found in our literature review. This study aimed to examine the impact of diverse wastes, i.e., marble dust (MD), paddy straw fiber (PSF), and bagasse ash (BA), on the mechanical attributes of unfired admixed adobe blocks, followed by modeling and optimization. The compressive strength of the admixed adobe blocks was evaluated in previous research [15] using varied contents of MD, BA, and 75 mm PSF. In this investigation, the split tensile strength test and flexural test were performed to determine the mechanical parameters of unfired admixed soil blocks. The marble dust was composed of a sufficient quantity of CaO, and the bagasse ash was composed primarily of SiO_2, as shown in the section of materials and methods. which results in pozzolanic action on treatment with water. The addition of paddy straw fiber in conjunction with marble dust and bagasse ash results in reduced water absorption and linear shrinkage of the unfired admixed soil blocks. This study helps to providing an of alternative solution to the disposal problem of bagasse ash, marble dust, and paddy straw fiber, hence reducing the environmental pollution. These unfired admixed soil blocks could be used in paving roads, footpaths adjacent to roads, and pavement, for petrol pumps made with the help of lock tiles.

It was the primary objective of the study to determine the mechanical performance of soil blocks admixed with marble dust, paddy straw fiber, and bagasse ash. To estimate the mechanical properties of the material, flexural strength, tensile strength, and efflorescence tests were performed. SEM and SEM-EDS were used to analyze the microstructures of the different samples in order to discuss and verify the experimental results. The results were analyzed using linear regression, and optimized values were calculated based on the modeling equations.

2. Materials and Methods

2.1. Materials

The soil for this investigation was collected in Gharuan, Kharar (Punjab), India. Table 1 shows the engineering characteristics of the soil sample. The PSF was obtained from agricultural land in Gharuan near Chandigarh University. Paddy straw fibers (PSF) were chopped into lengths of 75 mm, 100 mm, and 125 mm. Paddy straw with an average width of 2 mm was employed in the study.

Table 1. Clayey soil properties.

Soil Properties	Specific Gravity	Optimum Moisture Content (%)	Liquid Limit (%)	Plasticity Index (%)	Plastic Limit (%)	Maximum Dry Density (kg/m^3)	Unified Soil Classification System
Value	2.66	19	42.3	19.1	23.2	1670	CI

Table 2 demonstrates the XRF chemical composition of the marble dust powder, showing that the marble dust is mainly composed of calcium oxide (CaO). The specific gravity of the marble dust used for the study was 2.71.

Table 2. Chemical characteristics of marble dust.

Constituents	SiO_2	Al_2O_3	Fe_2O_3	CaO	MgO	SO_3	Na_2O	K_2O	P_2O_5	Cl^-	SrO	L.O. I
% age	0.78	0.22	0.07	54.82	0.26	0.25	0.11	0.03	0.05	0.06	0.05	43.22

The marble dust was tested by X-ray diffractogram to gather information regarding its mineralogical constituents, with the results shown in Figure 1. The typical peak of Bustamite (Ca O.228 Mn O.772 SiO_3), which is the major element of carbonate rocks, is denoted by the black colour. This result supports the information in Table 2 from the chemical analysis of the substance.

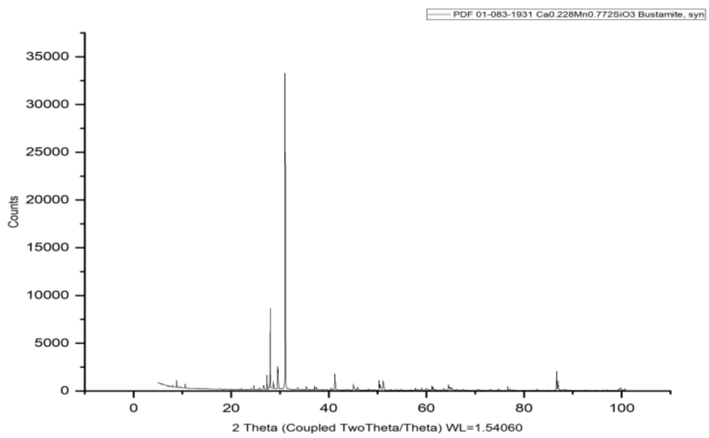

Figure 1. X-ray diffractogram (XRD) of marble dust.

Table 3 shows the chemical characteristics of bagasse ash (BA) as determined by X-Ray Fluorescence test. In Table 3, it is shown that BA is mainly composed of silicon oxide (SiO2) and lower contents of Calcium Oxide (CaO), Potassium Oxide (K2O), and Magnesium Oxide (MgO). The specific gravity of the BA used for the study was 1.92.

Table 3. SCBA chemical composition.

Constituents	SiO_2	MgO	Fe_2O_3	Na_2O	K_2O	CaO	Al_2O_3	SO_3	P_2O_5	Other Oxides
% age	74.14	3.68	1.73	0.51	5.67	4.65	2.32	1.69	4.37	1.24

The X-ray diffractogram information regarding the mineralogical constituents of sugarcane bagasse ash is shown in Figure 2. It can be observed that the sugarcane bagasse ash is richer in mineralogical constituents, with a majority of Tridymite (SiO_2) denoted by the red colour, followed by Silicalith-1 (96SiO2.xIBr) denoted by blue and Silicalite-1 (96SiO2.xICl) denoted by green. This result supports the information in Table 3 from the chemical analysis of the substance.

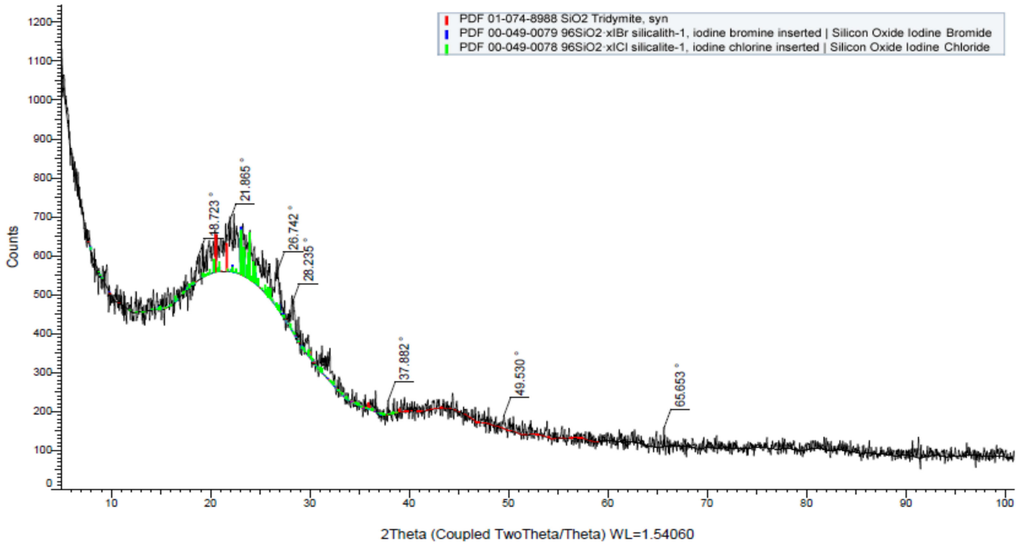

Figure 2. X-ray diffractogram (XRD) of bagasse ash.

2.2. Methodology

A design mix was created to test the impact of admixtures on the characteristics of soil blocks, as listed in Table 4. Bagasse ash content ranged from 7.5% to 12.5%, marble dust level ranged from 25% to 35%, and content of paddy straw fibre ranged from 0.8 percent to 1.2% by soil dry weight. The length of the paddy straw fiber was varied, at 75 mm, 100 mm, and 125 mm. It has been demonstrated that when 30% soil is replaced with marble dust, compressive strength is maximized [11]; however, no previous study of marble dust addition of 25% or 35% in soil blocks has been identified. For bagasse ash, while 10% soil replacement has shown the greatest results [16,17], there has been no research on the use of paddy straw fibre; based on research on other natural fibres, 1% fibre content and a length of 100 mm produced superior results [6,8]. Thus 0.8%, 1%, and 1.2% fibre content were added to different mixtures.

Table 4. Design mix using marble dust, paddy straw fibre, and bagasse ash in soil blocks.

Paddy Straw Fiber Length (mm) X1	Paddy Straw Fiber Content (%) X2	Bagasse Ash (%) - X3	Marble Dust (%) X4
75	0.8	7.5	25
100	1	10	30
125	1.2	12.5	35

The soil was prepared according to BIS [18]. All the materials were mixed in a trolley using a step-by-step process. Then, for the specific experimental design mix, according to the OMC acquired from the proctor compaction test, 50% of the water was added, then the remaining water was added with thorough mixing. A block size of 230 × 100 × 100 mm was employed in this investigation. These solid blocks were manufactured with the help of a machine, shown in Figure 3, which generated four unfired admixed adobe blocks per pressing.

Figure 3. Admixed adobe block manufacturing machine.

The final unfired admixed adobe blocks were in finished form after 28 days of curing, as shown in Figure 4, and were then used for further testing of the mechanical parameters. Curing of the blocks was performed by sprinkling them with water and then covering them with a jute bag until the next cycle of curing.

Figure 4. Unfired admixed adobe blocks.

IS 5816:1999 was used to perform the split tensile strength test. The compressive strength of a cylindrical soil block measured along its length is called the split tensile strength (STS). A cylindrical block with an L/D ratio of 2 was utilised for this test. Each mix was tested three times, and the average was used to determine the final outcome. A total of 243 specimens were created from 81 combinations. Equation (1) was used to compute the final split tensile strength, where P is the load, D is the diameter of specimen, and L is the height of specimen.

$$STS = \frac{2P}{\pi DL} \tag{1}$$

The flexural strength of a soil admixed block indicates the maximum stress it has been subjected to immediately before yielding. The flexural strength test was carried out according to standard code IS 4332(6):1972 (reaffirmed 2010). To initiate the testing process, an unfired admixed soil beam with dimensions 100 × 100 × 300 mm, as shown in Figure 5, was brush cleaned and placed in the testing machine. The maximum load at which the first crack appeared in the beam was noted and termed as P. Subsequently, the value of FS was calculated using Equation (2), where *l* is the span between lower supports (mm), *b* is the width of the beam (mm), and *d* is the depth of the beam (mm).

$$R = 3\left(\frac{Pl}{bd^2}\right) \quad (2)$$

Figure 5. Specimens for flexural strength test.

In this study, the efflorescence test was conducted on the blocks as per IS 3495 (part 3):1992 [19] and IS 5454-1978. When water is present in brick, stone, concrete, stucco, or other construction surfaces, efflorescence is developed as a crystalline coating of salts consisting of salt deposits with a greyish or white colour left on the surface after water evaporates. The unfired admixed soil block specimens were immersed in a dish containing water up to depth of 25 mm. When the water had been absorbed and the specimens appeared to be dry, a similar quantity of water was added to the dish and efflorescence was observed after the water evaporated again. The observed results were reported as per standard codes.

3. Results and Discussions

3.1. *Split Tensile Strength (TS) of Unfired Admixed Soil Block*

In this section, we describe the results of our study of the effects of MD and BA on the split tensile strength of adobe block admixed with 0.8 percent PSF with a length of 75 mm (shown in Figure 6). It was found that tensile strength showed an increment with increase in marble dust at constant bagasse ash content. At 25% MD and 7.5% BA, the tensile strength of the admixed adobe block reinforced with paddy straw fiber was 0.36 MPa, which increased to 0.44 MPa with 7.5% bagasse ash and 35% marble dust. A similar trend was observed for 10% bagasse ash and 12.5% bagasse ash. However, it was observed from the experimental results that tensile strength showed an increment with increase in bagasse ash until 10% bagasse ash, then gradually decreased towards 12.5% bagasse ash at constant marble dust content. At 35% marble dust and 7.5% bagasse ash, the tensile strength of the admixed adobe block reinforced with paddy straw fiber was 0.44 MPa, which increased to 0.49 MPa with 10% bagasse ash and decreased to 0.47 MPa with 12.5% bagasse ash and 35% marble dust. A similar trend was observed for 25% marble dust and 30% marble dust.

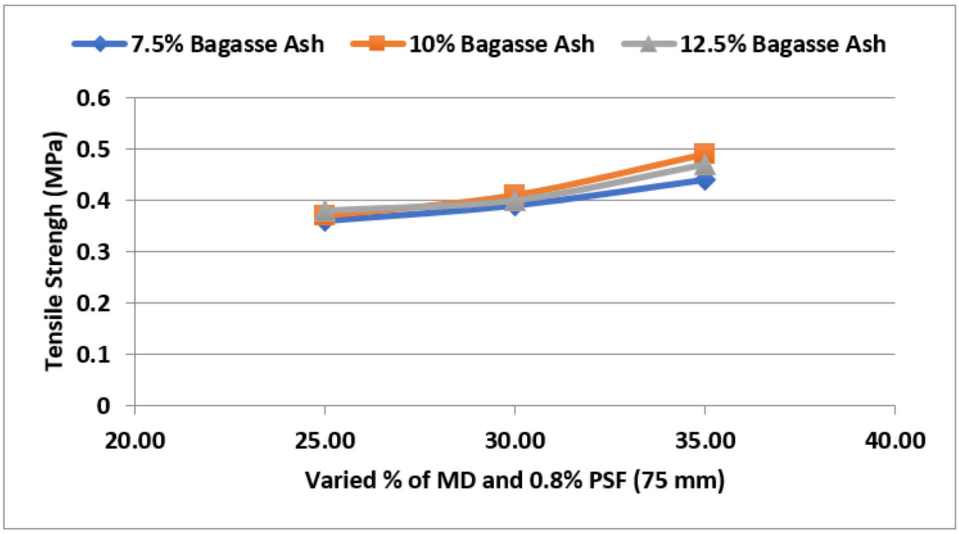

Figure 6. Effect of MD and BA on tensile strength of block reinforced with 0.8% PS fiber (75 mm).

In addition, the effect of MD and BA on the tensile strength of adobe block admixed with 1% paddy straw fiber with a length of 75 mm is shown in Figure 7. It was found that tensile strength showed an increment with increase in marble dust until 30% marble dust was reached, then gradually decreased towards 35% marble dust at constant bagasse ash content. At 25% MD and 7.5% BA, the tensile strength of the admixed adobe block reinforced with paddy straw fiber was 0.39 MPa, which increased to 0.48 MPa with 7.5% bagasse ash and 30% marble dust and then decremented to 0.47 MPa with 7.5% bagasse ash and 35% marble dust. A similar trend was observed for 10% bagasse ash and 12.5% bagasse ash. However, it was observed from the experimental results that tensile strength showed an increment with increase in bagasse ash until 10% bagasse ash was reached, then gradually decreased towards 12.5% bagasse ash at constant marble dust content. At 35% marble dust and 7.5% bagasse ash, the tensile strength of the admixed adobe block reinforced with paddy straw fiber was 0.47 MPa, which increased to 0.5 MPa with 10% bagasse ash and decreased to 0.49 MPa with 12.5% bagasse ash and 35% marble dust. A similar trend was observed for 25% marble dust and 30% marble dust. In addition, the effect of MD and BA on the tensile strength of adobe block admixed with 1.2 percent PSF of length 75 mm is shown in Figure 8. It was found that tensile strength showed an increment with increase in marble dust until 30% marble dust was reached, then gradually decreased towards 35% marble dust at constant bagasse ash content. At 25% MD and 7.5% BA, the tensile strength of the admixed adobe block reinforced with paddy straw fiber was 0.37 MPa, which increased to 0.45 MPa with 7.5% bagasse ash and 30% marble dust and then decremented to 0.44 MPa with 7.5% bagasse ash and 35% marble dust. A similar trend was observed for 10% bagasse ash and 12.5% bagasse ash. However, it was observed from the experimental results that tensile strength showed an increment with increase in bagasse ash until 10% bagasse ash was reached, then gradually decrease towards 12.5% bagasse ash at constant marble dust content. At 35% marble dust and 7.5% bagasse ash, the tensile strength of the admixed adobe block.

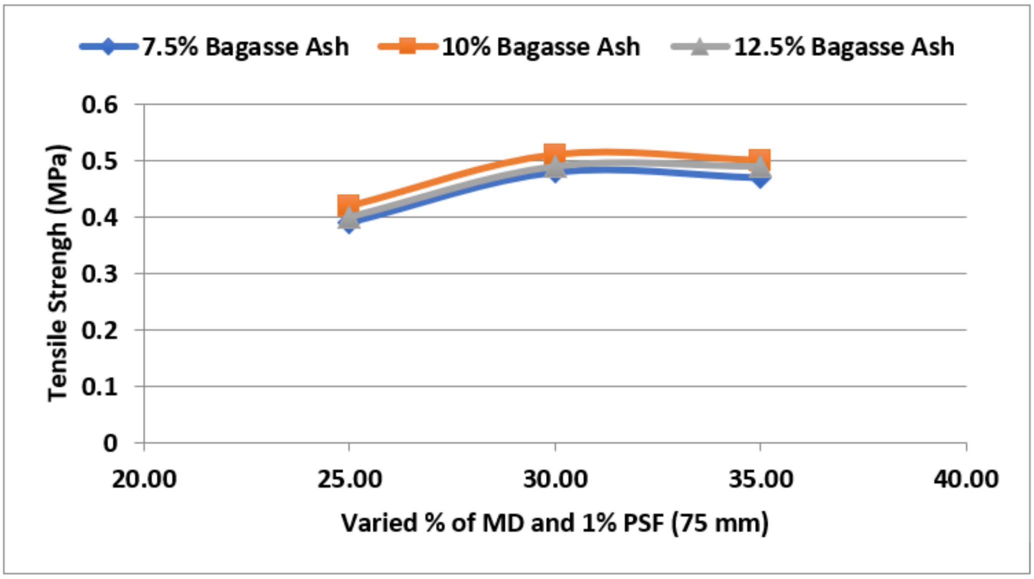

Figure 7. Effect of MD and BA on tensile strength of block reinforced with 1% PS fiber (75 mm).

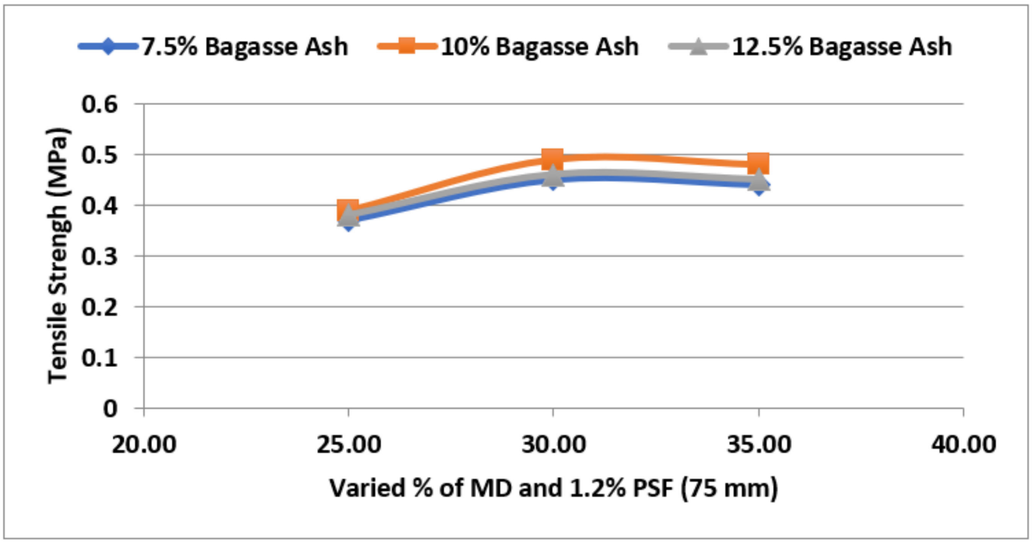

Figure 8. Effect of MD and BA on tensile strength of block reinforced with 1.2% PS fiber (75 mm).

Reinforced with paddy straw fiber was 0.44 MPa, which increased to 0.48 MPa with 10% bagasse ash and then decreased to 0.45 MPa with 12.5% bagasse ash and 35% marble dust. A similar trend was observed for 25% marble dust and 30% marble dust. The inclusion of fibre that reinforces the soil matrix, improving the tensile strength of the blocks, which is typically not a distinctive measure of the performance of the soil block. The metric is utilised in this study to emphasize the significance of fibre reinforcement in stiffening fibre-reinforced soil blocks. According to these findings, fibre incorporation improves the tensile strength of the soil blocks [14].

For 100 mm and 125 mm PSF, a similar effect of MD and BD on tensile strength was observed. As shown in Figure 9, at 25% MD and 7.5% BA the tensile strength of the admixed adobe block reinforced with 0.8% 100 mm paddy straw fiber was 0.41 MPa, which increased to 0.49 MPa with 7.5% bagasse ash and 35% marble dust.

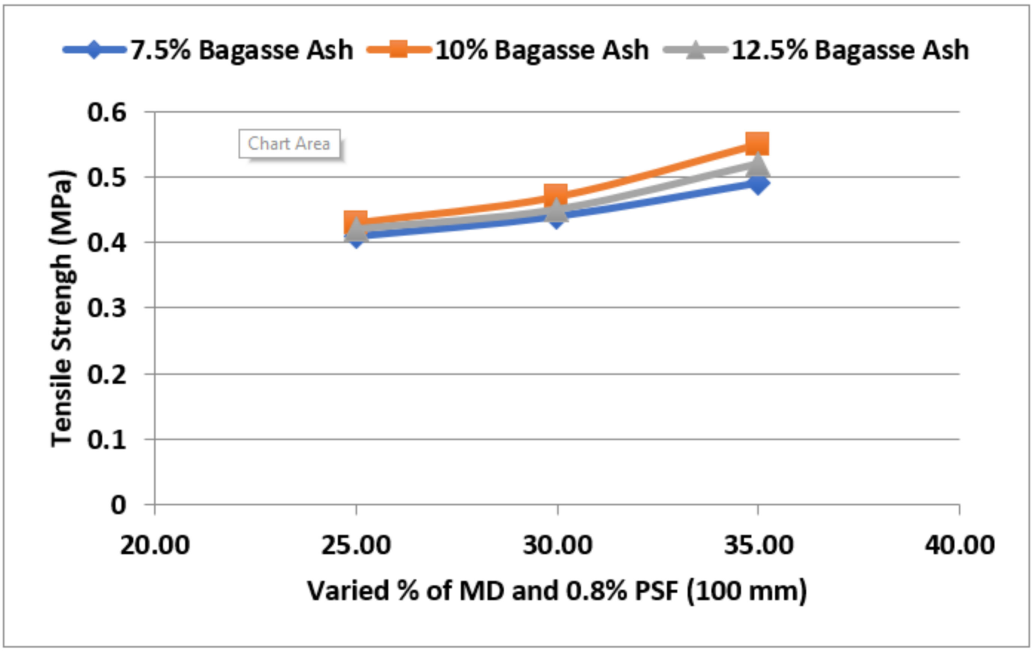

Figure 9. Effect of MD and BA on tensile strength of block reinforced with 0.8% PS fiber (100 mm).

In addition, the effect of MD and BA on the tensile strength of adobe block admixed with 1% and 1.2% paddy straw fiber of length 100 mm was studied, as shown in Figures 10 and 11, respectively. It was found that tensile strength showed a similar trend with these PSF contents.

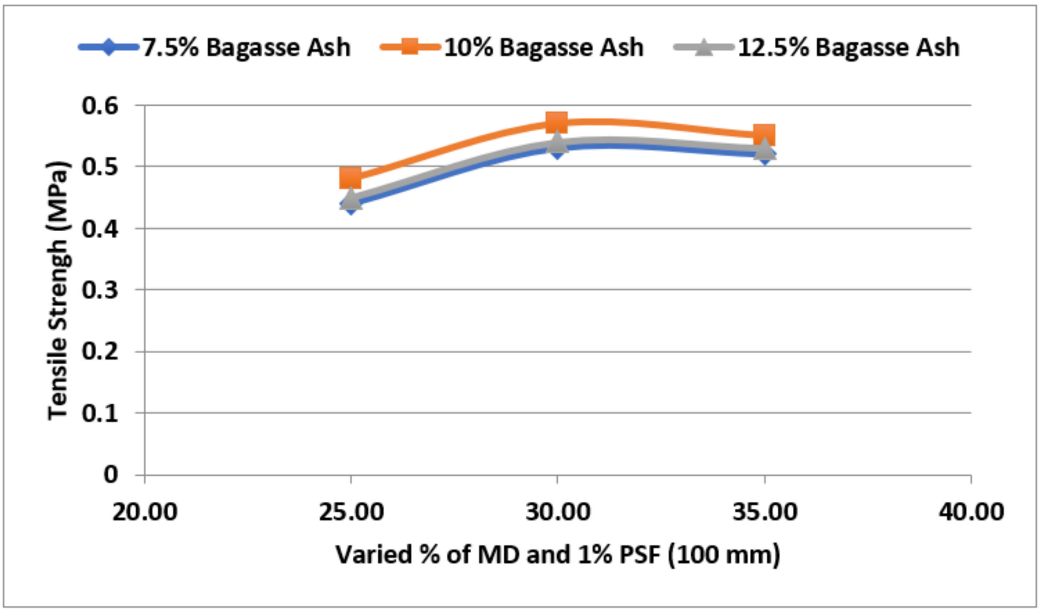

Figure 10. Effect of MD and BA on tensile strength of block reinforced with 1% PS fiber (100 mm).

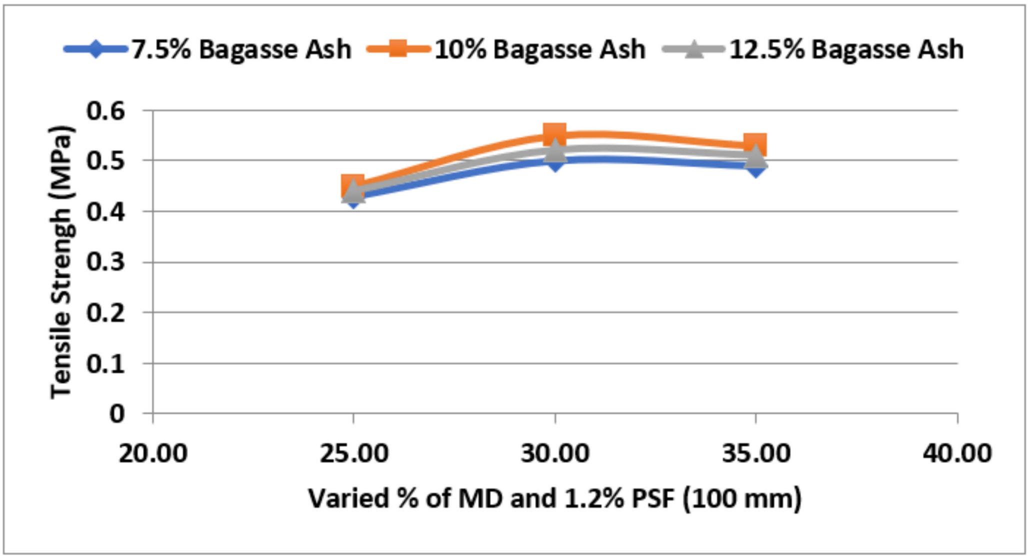

Figure 11. Effect of MD and BA on tensile strength of block reinforced with 1.2% PS fiber (100 mm).

Further, the effect of MD and BA on the split tensile strength of adobe block admixed with 0.8 percent PSF of length 125 mm is shown in Figure 12. It was found that tensile strength showed an increment with increase in marble dust at constant bagasse ash content. However, it showed an increment with increase in bagasse ash until 10% bagasse ash, then gradually decreased towards 12.5% bagasse ash at constant marble dust content.

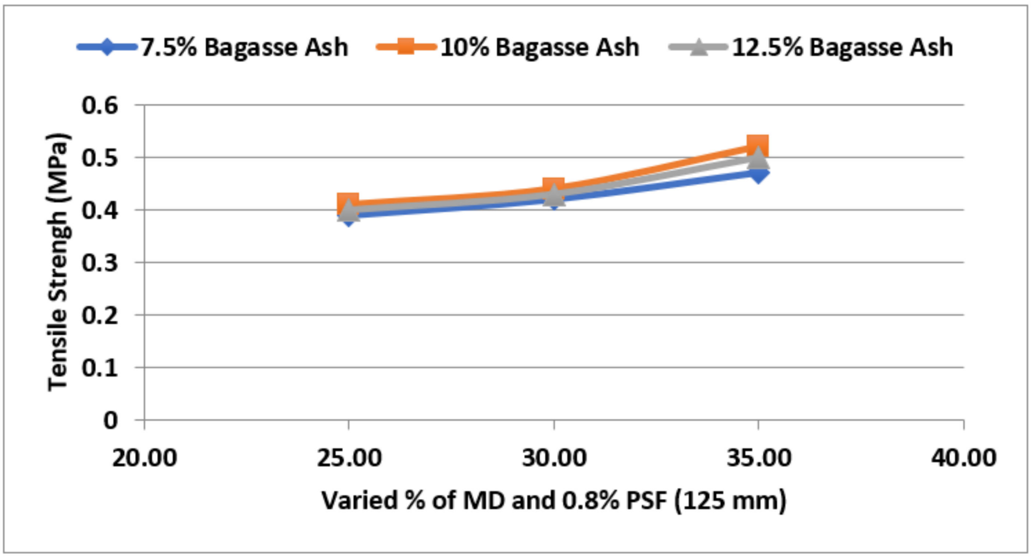

Figure 12. Effect of MD and BA on tensile strength of block reinforced with 0.8% PS fiber (125 mm).

In addition, the effect of MD and BA on the tensile strength of adobe block admixed with 1% and 1.2% paddy straw fiber of length 125 mm is shown in Figures 13 and 14, respectively. It was found that tensile strength showed a similar trend with these PSF contents.

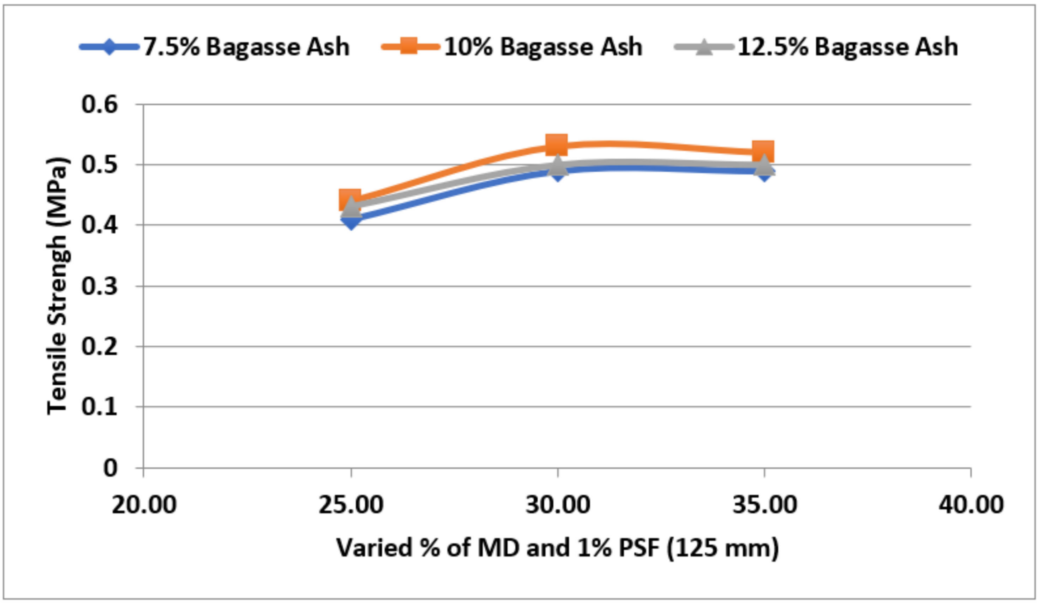

Figure 13. Effect of MD and BA on tensile strength of block reinforced with 1% PS fiber (125 mm).

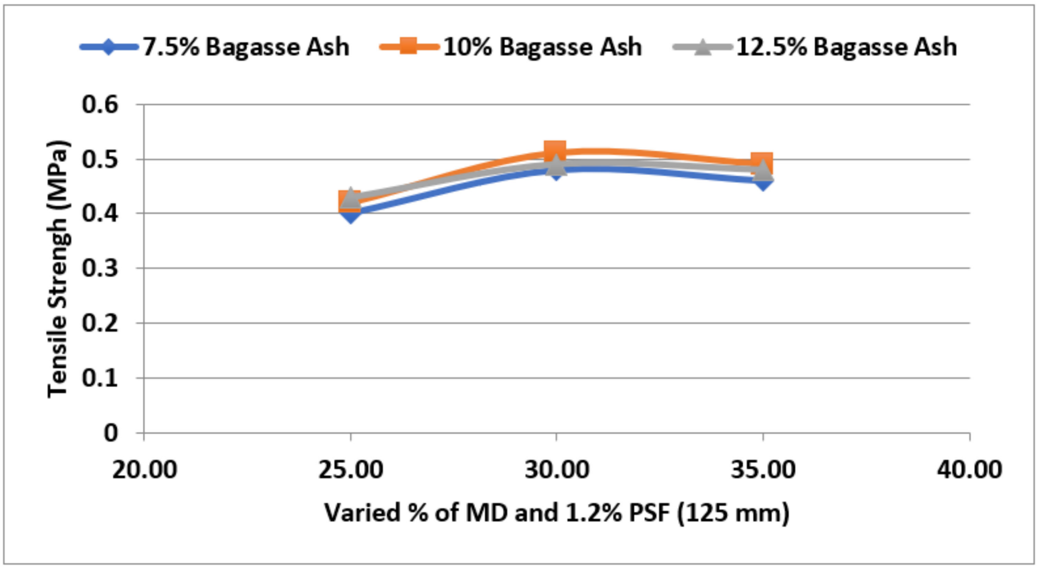

Figure 14. Effect of MD and BA on tensile strength of block reinforced with 1.2% PS fiber (125 mm).

3.2. Flexural Strength of Unfired Admixed Soil Block

In this section, the effect of MD and BA on the flexural strength of adobe block admixed with 0.8 percent PSF of length 75 mm was studied, as shown in Figure 15. It was discovered that flexural strength showed a rising trend with increasing marble dust at constant bagasse ash content. At 25% MD and 7.5% BA, the flexural strength of the adobe block reinforced with paddy straw fiber was 0.25 MPa, which increased to 0.3 MPa with 7.5% bagasse ash and 35% marble dust. A similar trend was observed for 10% bagasse ash and 12.5% bagasse ash. Moreover, a similar trend was observed with an increase in bagasse ash for constant marble dust content. At 25% MD and 7.5% BA, the flexural strength of the adobe block reinforced with paddy straw fiber was 0.25 MPa, which increased to 0.31 MPa with 12.5% bagasse ash and 25% marble dust. A similar trend was observed for 30% marble dust and 35% marble dust. This might be due to the soil/marble dust/sugarcane bagasse ash/paddy straw fiber matrix gradually densifying as a result of hydration and pozzolanic processes [16].

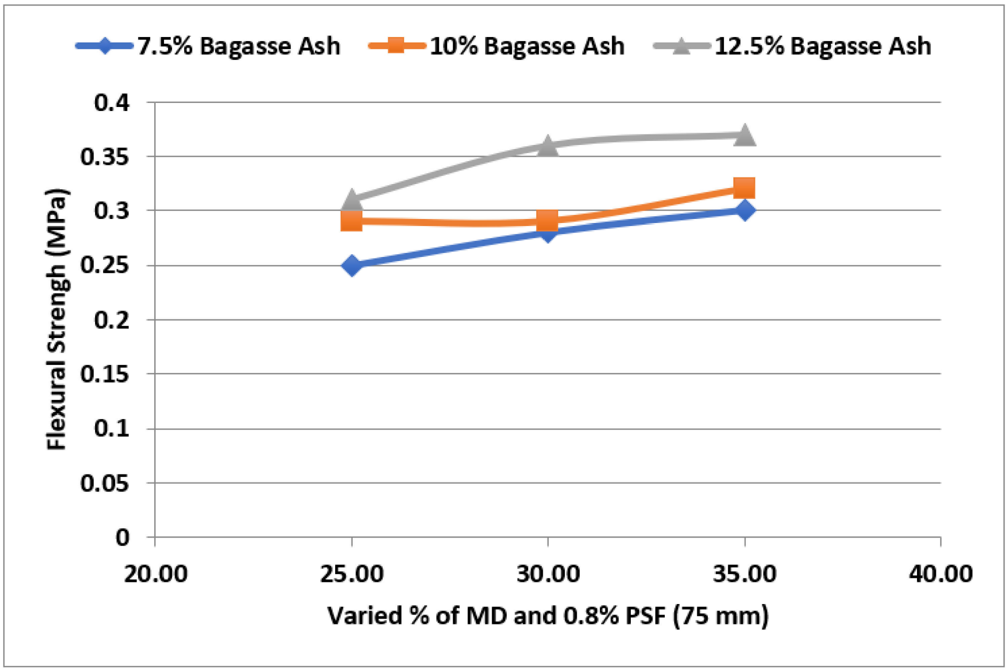

Figure 15. Effect of MD and BA on flexural strength of block reinforced with 0.8% PS fiber (75 mm).

The effect of MD and BA on the flexural strength of adobe block admixed with 1% paddy straw fiber of length 75 mm is shown in Figure 16. It was discovered that flexural strength showed a rising trend with increasing marble dust at constant bagasse ash content. At 25% MD and 7.5% BA, the flexural strength of the adobe block reinforced with paddy straw fiber was 0.24 MPa, which increased to 0.28 MPa with 7.5% bagasse ash and 35% marble dust. A similar trend was observed for 10% bagasse ash and 12.5% bagasse ash. Moreover, a similar trend was observed with increasing bagasse ash for constant marble dust content. At 25% MD and 7.5% BA, the flexural strength of the adobe block reinforced with paddy straw fiber was 0.24 MPa, which increased to 0.3 MPa with 12.5% bagasse ash and 25% marble dust. A similar trend was observed for 30% marble dust and 35% marble dust.

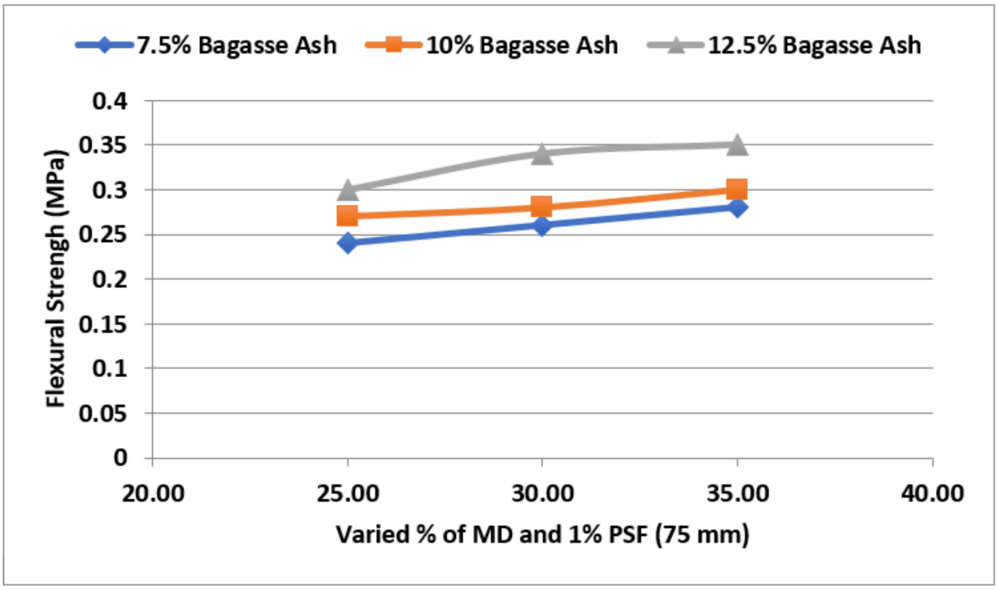

Figure 16. Effect of MD and BA on flexural strength of block reinforced with 1% PS fiber (75 mm).

The effect of MD and BA on the flexural strength of adobe block admixed with 1.2 percent PSF of length 75 mm is shown in Figure 17. Flexural strength showed a rising trend with increasing marble dust at constant bagasse ash content. At 25% MD and 7.5% BA, the flexural strength of the adobe block reinforced with paddy straw fiber was 0.18 MPa, which increased to 0.21 MPa with 7.5% bagasse ash and 35% marble dust. A similar trend was observed for 10% bagasse ash and 12.5% bagasse ash. Moreover, a similar trend was observed with increased bagasse ash for constant marble dust content.

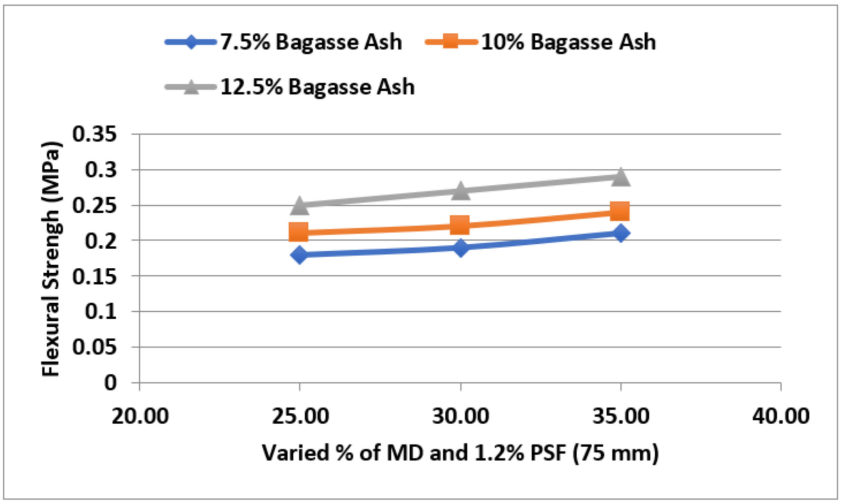

Figure 17. Effect of MD and BA on flexural strength of block reinforced with 1.2% PS fiber (75 mm).

At 25% MD and 7.5% BA, the flexural strength of the adobe block reinforced with paddy straw fiber was 0.18 MPa, which increased to 0.25 MPa with 12.5% bagasse ash and 25% marble dust. A similar trend was observed for 30% marble dust and 35% marble dust. The possibility for additional fiber–fiber interactions rose when fibre content exceeded 0.8 percent, reducing the production of fiber–matrix and matrix–matrix connections and resulting in flexural strength loss [20–22]. In addition, for 100 mm and 125 mm PSF, a similar effect of MD and BD on flexural strength was observed. As shown in Figure 18, at 25% MD and 7.5% BA the flexural strength of the adobe block reinforced with paddy straw fiber was 0.27 MPa, which increased to 0.31 MPa with 7.5% bagasse ash and 35% marble dust. A similar trend was observed for 10% bagasse ash and 12.5% bagasse ash.

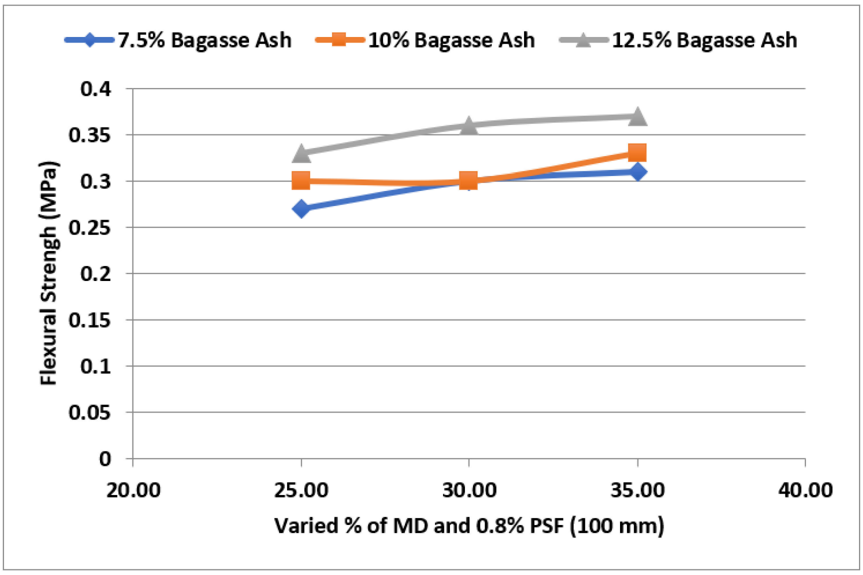

Figure 18. Effect of MD and BA on flexural strength of block reinforced with 0.8% PS fiber (100 mm).

The effect of MD and BA on the flexural strength of adobe block admixed with 1% and 1.2% paddy straw fiber of length 100 mm is shown in Figures 19 and 20, respectively. It was found that FS showed a similar trend with these PSF contents.

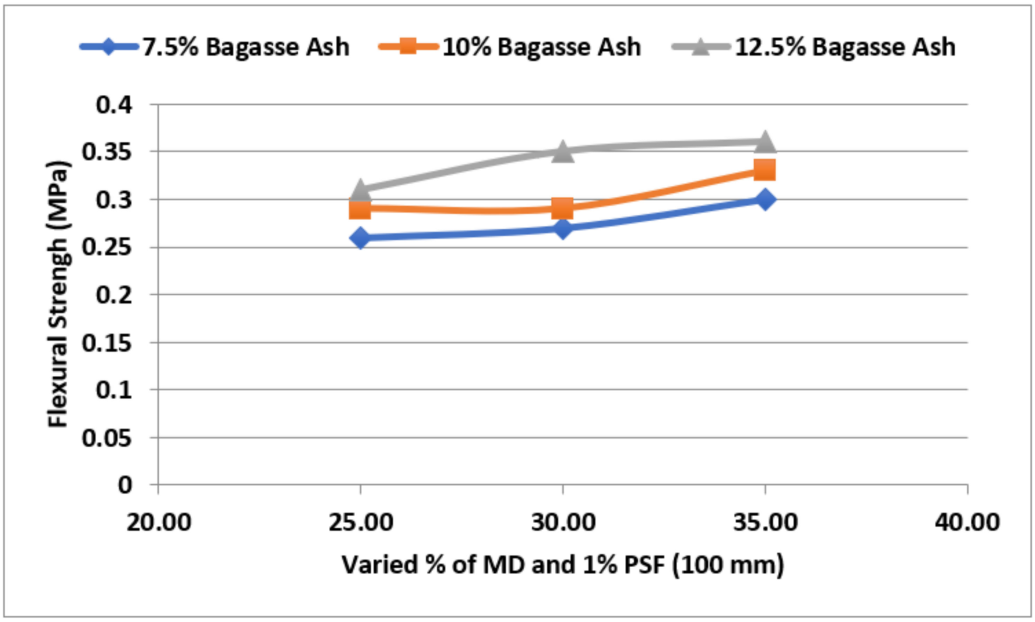

Figure 19. Effect of MD and BA on flexural strength of block reinforced with 1% PS fiber (100 mm).

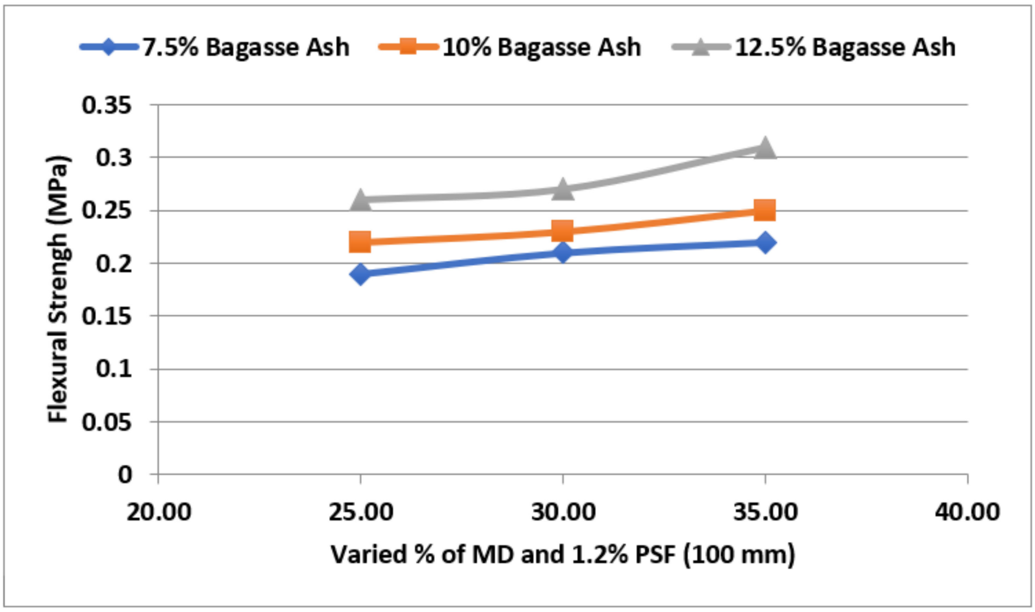

Figure 20. Effect of MD and BA on flexural strength of block reinforced with 1.2% PS fiber (100 mm).

Further, the effect of MD and BA on the flexural strength of adobe block admixed with 0.8 percent PSF of length 125 mm is shown in Figure 21. It was discovered that flexural strength showed a rising trend with increasing marble dust at constant bagasse ash content. Moreover, a similar trend was observed with increased bagasse ash for constant marble dust content.

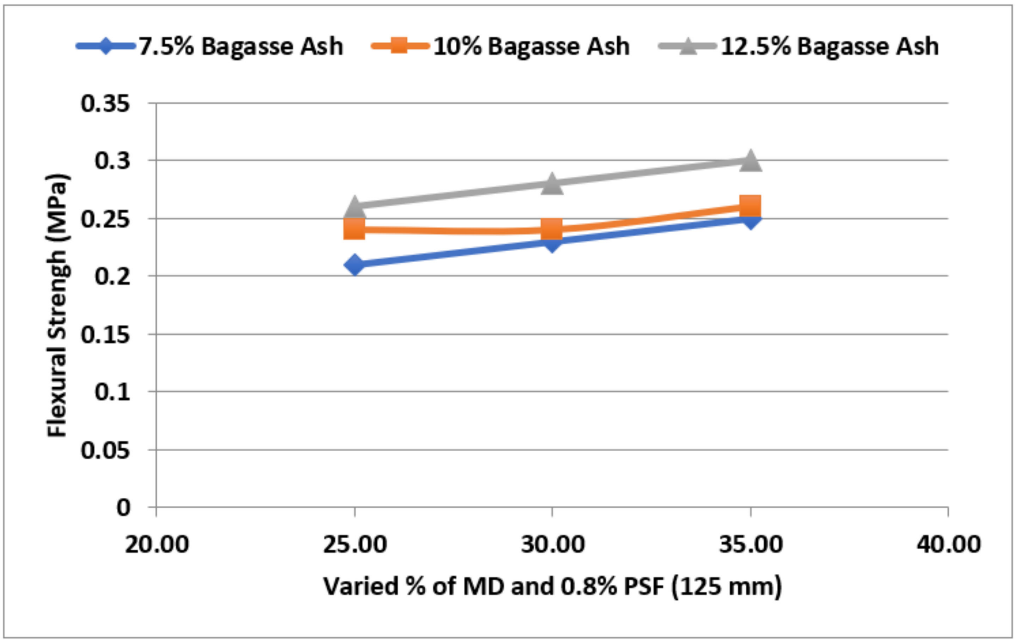

Figure 21. Effect of MD and BA on flexural strength of block reinforced with 0.8% PS fiber (125 mm).

The effect of MD and BA on the flexural strength of adobe block admixed with 1% and 1.2% paddy straw fiber of length 125 mm is shown in Figures 22 and 23, respectively. It was found that FS showed a similar trend with these PSF contents.

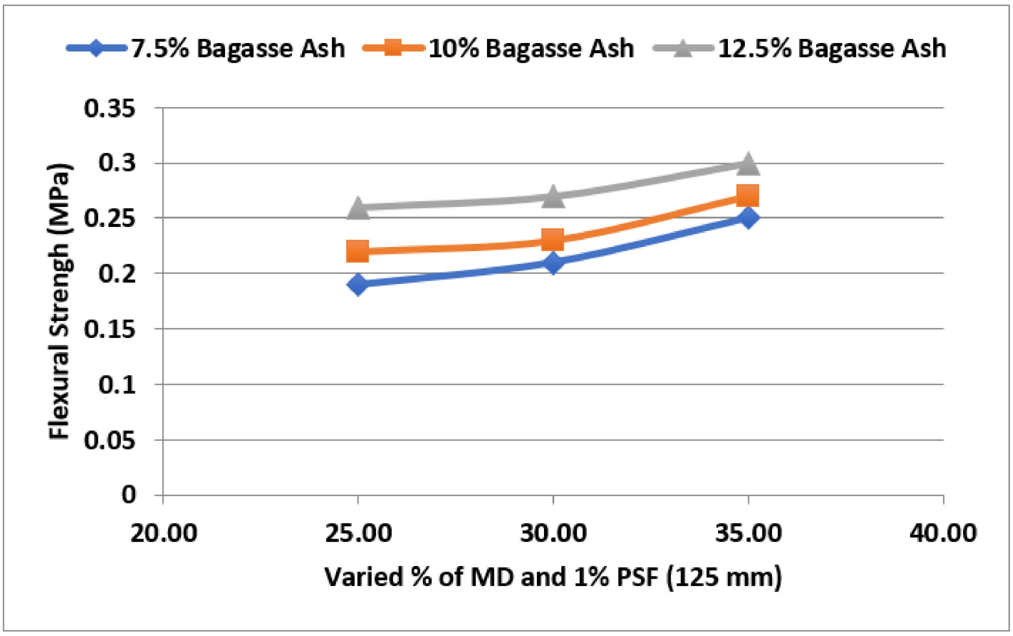

Figure 22. Effect of MD and BA on flexural strength of block reinforced with 1% PS fiber (125 mm).

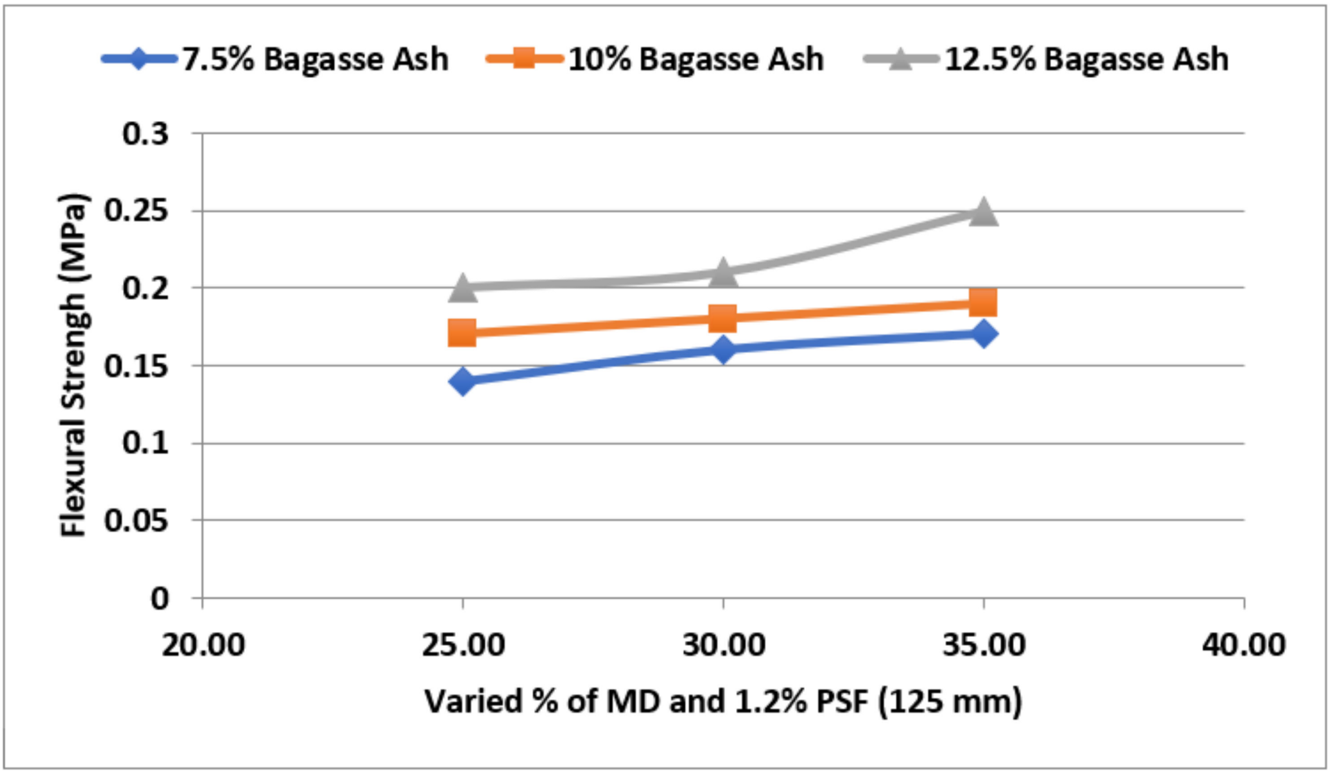

Figure 23. Effect of MD and BA on flexural strength of block reinforced with 1.2% PS fiber (125 mm).

3.3. Efflorescence of Unfired Admixed Soil Block

In this study, efflorescence testing was conducted on blocks as per IS 3495 (part 3):1992 and IS5454-1978. There was no efflorescence on any of the tested combinations [23–25].

3.4. Statistical Analysis

3.4.1. Model Equation: Split Tensile Strength versus X1, X2, X3, X4

The association between parameters and TS was developed using regression analysis, and the results are shown in Equation (3). The following model equation was used to determine the TS of unfired soil blocks admixed with varied proportions of PSF, MD, and BA:

$$\begin{gathered}TS = -2.879 + 0.01403X1 + 1.944X2 + 0.0787X3 + 0.0776X4 - 0.000065\, X1{*}X1 - 0.824\, X2{*}X2 - 0.003941\, X3{*}X3 - \\ 0.001030\, X4{*}X4 - 0.000111\, X1{*}X2 + 0.000009\, X1{*}X3 - 0.000016\, X1{*}X4 - 0.00111\, X2{*}X3 - 0.00722\, X2{*}X4 + \\ 0.000111\, X3{*}X4.\end{gathered} \tag{3}$$

Here, X1, X2, X3, and X4 represent the parameters, i.e., the length of PSF and proportions of PSF, SCBA, and MD. The residual plots of TS are shown in Figure 24, where the independent variable is on the horizontal axis and the residuals are displayed on the vertical axis. The R^2 value of 89.96% was obtained through statistical analysis.

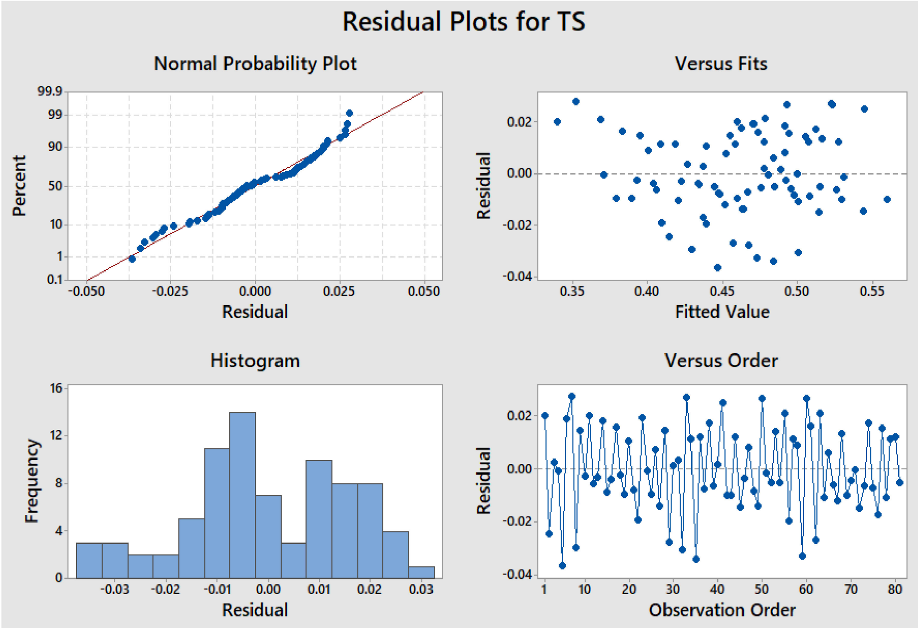

Figure 24. Residual plots of tensile strength.

3.4.2. Model Equation: Flexural Strength versus X1, X2, X3, X4

The association between the parameters and FS was developed using regression analysis, and the results are shown in Equation (4). The following model equation was used to determine FS of unfired soil blocks admixed with varied proportion of PSF, MD, and BA:

$$FS = -0.567 + 0.010737\ X1 + 0.999\ X2 - 0.02156\ X3 - 0.00319\ X4 - 0.000058\ X1 * X1 - 0.6343\ X2 * X2 + 0.001541\ X3 * X3 + 0.000119\ X4 * X4 + 0.000611\ X1 * X2 - 0.000058\ X1 * X3 - 0.000002\ X1 * X4 + 0.00556\ X2 * X3 - 0.00111\ X2 * X4 + 0.000133\ X3 * X4. \quad (4)$$

Here, X1, X2, X3, and X4 represent the parameters, i.e., the length of PSF and proportions of PSF, SCBA, and MD. The residual plots of FS are shown in Figure 25, where the independent variable is on the horizontal axis and the residuals are displayed on the vertical axis. The R^2 value of 98.26% was obtained through statistical analysis.

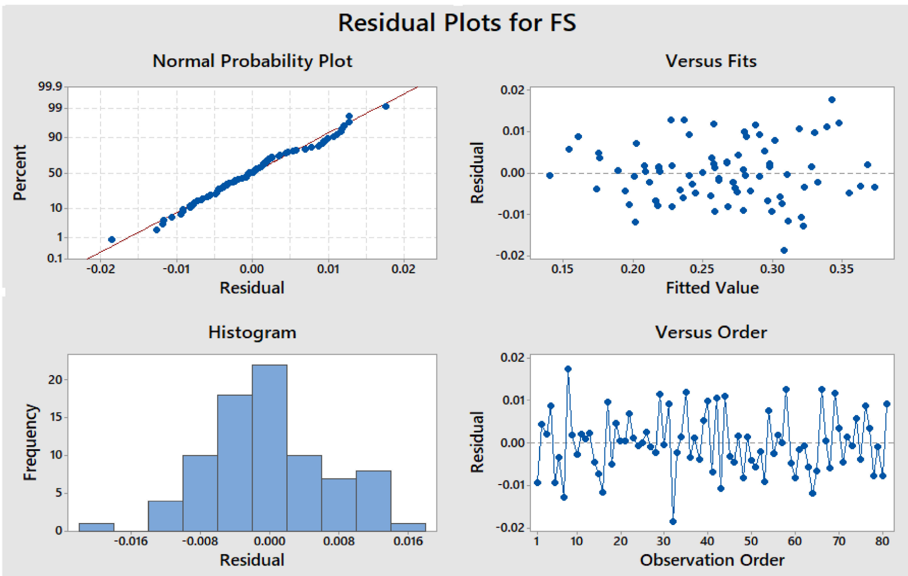

Figure 25. Residual plots of flexural strength.

3.5. Optimization

The values of the response factors, i.e., TS and the parameters at optimized conditions, are shown in Table 5. From the table, it can be observed that the optimum value of TS, i.e., 0.56 Mpa, is achieved by the unfired soil block admixed with 104 mm length and 1% PSF, 10% BA, and 35% MD.

Table 5. Optimized value of TS for various parameters at optimized conditions.

Response Factor/Parameter	PSF Length (mm)	PSF Content (%)	SCBA Content (%)	MD Content (%)	Optimum Value of Response Factor
	X1	**X2**	**X3**	**X4**	
Tensile Strength	104	1	10	35	0.56

Similarly, the values of the response factors, i.e., FS and the parameters at optimized conditions, are shown in Table 6. From the table, it can be observed that the optimum value of FS, i.e., 0.39 MPa, is achieved by the unfired soil block admixed with 90 mm length and 0.85% PSF, 12.5% BA, and 35% MD.

Table 6. Optimized value of FS for various parameters at optimized conditions.

Response Factor/Parameter	PSF Length (mm)	PSF Content (%)	SCBA Content (%)	MD Content (%)	Optimum Value of Response Factor
	X1	**X2**	**X3**	**X4**	
Flexural Strength	90	0.85	12.5	35	0.39

3.6. SEM (Scanning Electron Microscopy Analysis)

In this study, SEM (Scanning Electron Microscope) testing was conducted to study the effect of bagasse ash and marble dust on the soil structure and soil–paddy straw fiber interface with the help of the SEM machine at UCRD, Chandigarh University [26–28]. SEM images are presented and discussed in this section. Figure 26 shows an SEM image of an unfired admixed adobe block specimen reinforced with paddy straw fiber with a length of 100 mm.

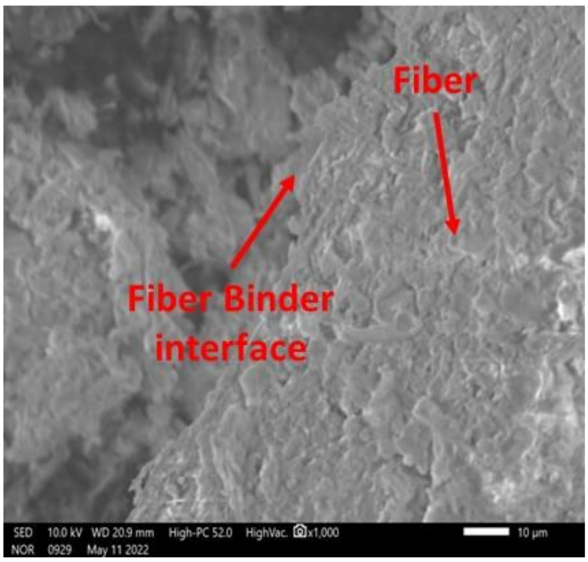

Figure 26. SEM image of specimen of unfired admixed adobe block reinforced with paddy straw fiber with length 100 mm (Bagasse ash: Marble Dust: Paddy straw fiber: 12.5%: 35%: 0.8%).

This specimen consisted of 12.5% Bagasse ash, 35% Marble Dust, and 0.8 percent PSF. For the SEM analysis, a very minute part of the specimen was taken and the soil mix adhered with fiber from the block was taken as a specimen for SEM analysis. It can be observed from the images that the soil–bagasse ash–marble dust mix was thoroughly adhered with the fiber [29–31]. Furthermore, the amount of pores is negligible, as can be seen from the image. These images support the results earlier results regarding the higher flexural and tensile strength of this sample.

Figure 27 shows an SEM image of an unfired admixed adobe block specimen reinforced with paddy straw fiber with a length of 125 mm. This specimen consisted of 7.5% Bagasse ash, 25% Marble Dust, and 1.2 percent PSF.

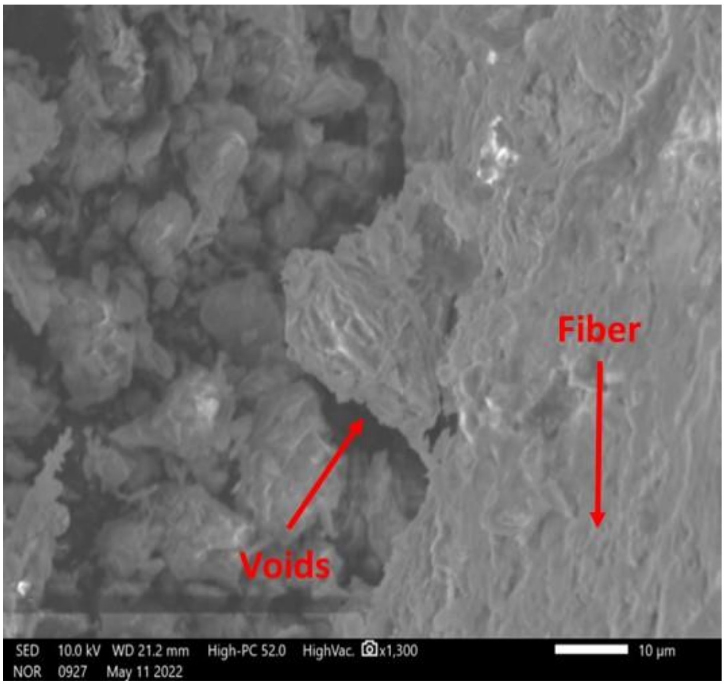

Figure 27. SEM image of specimen of unfired admixed adobe block reinforced with paddy straw fiber with length 125 mm (Bagasse ash: Marble Dust: Paddy straw fiber: 7.5%: 25%: 1.2%).

Again, a very minute part of the specimen was taken [21], and the soil mix adhered with fiber from the block was taken as the specimen for SEM analysis [32–34]. It can be observed from the image that the soil–bagasse ash–marble dust mix was not thoroughly adhered with the fiber. Furthermore, the pore content is higher, as can be seen from the image. These images support the earlier results regarding the lower flexural and tensile strength of this mixture.

3.7. EDS (Energy Dispersive X-ray Spectroscopy)

In this study, EDS (Energy Dispersive X-Ray Spectroscopy) testing was conducted to study the elemental analysis of a specimen [35–37]. This test provides the elemental composition of the surface of a specimen. Figure 28 shows an EDS image of a specimen of unfired admixed adobe block reinforced with paddy straw fiber with a length of 75 mm. This specimen consisted of 12.5% Bagasse ash, 30% Marble Dust, and 0.8 percent PSF. For the EDS analysis, a very minute part of the specimen was taken. The abscissa of the graph represents ionization energy and the ordinate represents the intensity (Count). Higher intensity of a particular element indicates that its presence is higher at that particular point [22,23]. It can be observed from Figure 28 that oxygen (O) and silica (Si) are the major elements detected on the surface, with Magnesium (Mg) and Aluminium (Al) detected in minor amounts.

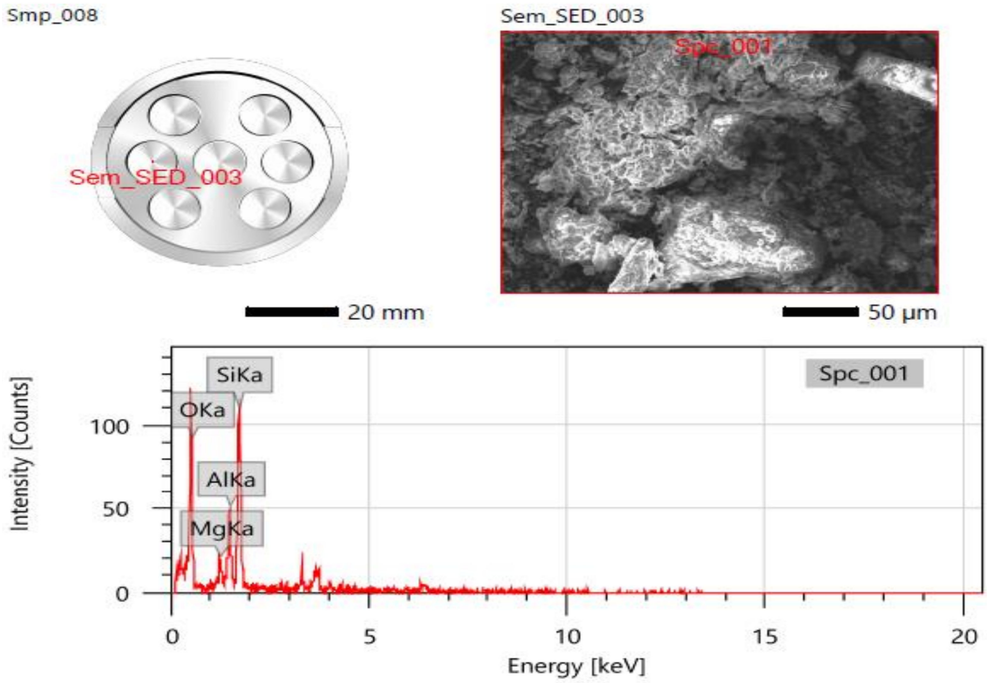

Figure 28. EDS of unfired admixed adobe block specimen reinforced with paddy straw fiber with length 75 mm (Bagasse ash: Marble Dust: Paddy straw fiber: 12.5%: 30%: 0.8%).

Figure 29 shows an EDS image of an unfired admixed adobe block specimen reinforced with paddy straw fiber with a length of 75 mm. This specimen consisted of 7.5% Bagasse ash, 25% Marble Dust, and 1.2 percent PSF. It can be observed from Figure 29 that oxygen (O) and silica (Si) are the major elements detected on the surface, along with a minor quantity of Aluminium (Al) [38–41].

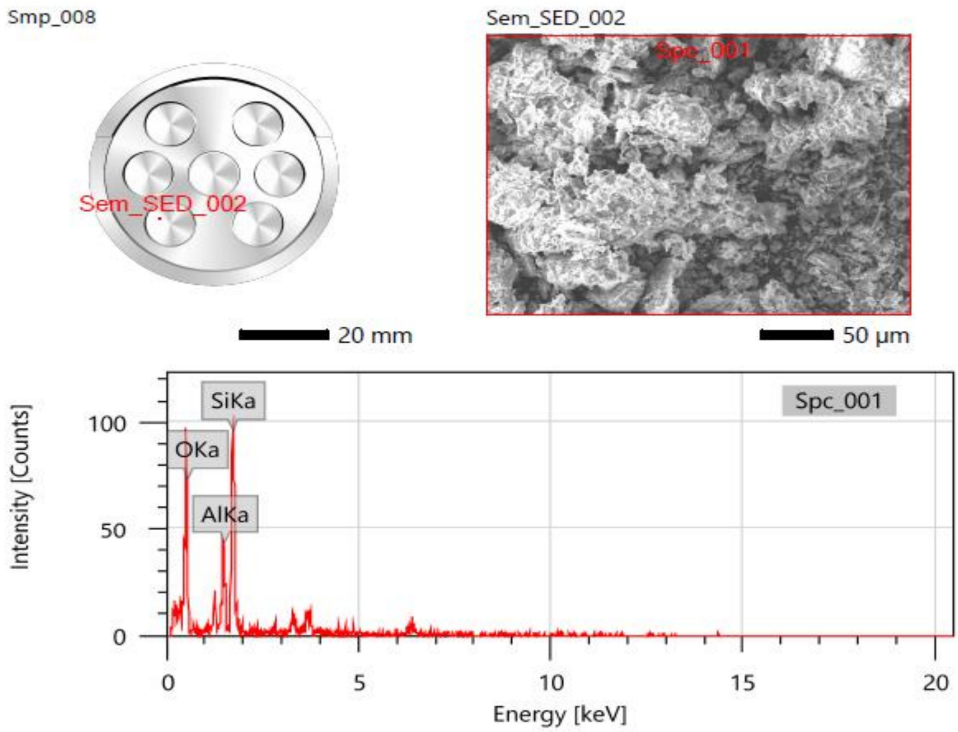

Figure 29. EDS of unfired admixed adobe block specimen reinforced with paddy straw fiber with length 75 mm (Bagasse ash: Marble Dust: Paddy straw fiber: 7.5%: 25%: 1.2%).

Thus, unfired admixed adobe blocks as a binder were chosen, as they have been used successfully for stabilizing clay for road constructions in low-temperature regions along with pavement engineering for improving slope stability. The rapid stabilization of a mix or slope is made possible by quicklime, which removes water from the stabilized mix or surrounding soil [33–35]. The use of adobe blocks admixed with cementitious binders is widely used in the construction of roads, pavement, and foundations. In addition to strengthening the soil against destructive weather forces, unfired admixed adobe blocks with the inclusion of waste materials contributed to improved strength and bearing capacity by reducing moisture movement, "rutting", and fatigue-cracking, imparting waterproofing characteristics, controlling volume stability against swell–shrink behavior caused by moisture changes, and enhancing erosion, weathering, and traffic load resistance [36–38]. Therefore, unfired admixed adobe blocks incorporating various waste materials are of interest to those involved in improving soil and geotechnical properties using industrial byproducts, such as civil and construction engineers, and engineering geologists [39–41].

4. Conclusions

This study's major objective was to determine the applicability of unfired soil blocks admixed with marble dust, paddy straw fiber, and bagasse ash from the perspective of mechanical attributes. Flexural strength, tensile strength, and efflorescence testing were performed to estimate the mechanical attributes of the blocks. Microstructural analysis was conducted on different samples using SEM and SEM-EDS in order to discuss and verify the results obtained experimentally. Further, linear regression analysis was performed on the results and the optimized values were calculated from the modeling equations using optimization techniques. The various conclusions drawn from these tests are discussed below:

(a) The split tensile strength (TS) was observed to rise with increasing MD for a fixed amount of BA and PSF. PSF and BA could be added as per the optimum values found by the model, while higher content reduces the TS of the block.
(b) The optimization process made it evident that the optimum value of TS was observed for soil blocks with 104 mm length and 1% PSF, 10% BA, and 35% MD, i.e., 0.56 MPa, which implies that addition of PSF increases the TS of the block.
(c) While estimating the flexural strength of the block, it was observed that FS rises with increasing MD for a fixed amount of BA and PSF. Similarly, with increasing BA for a fixed amount of MD and PSF, the FS of the soil block was found to be increase. The PSF could be added as per the optimum values found by the model, as any higher content reduces the FS of the blocks.
(d) On optimization, it was found that the optimum value of FS was observed for soil blocks with 90 mm length and 0.85% PSF, 12.5% BA, and 35% MD, i.e., 0.39 MPa, which implies that addition of PSF increases the PSF of the block.
(e) No efflorescence was observed on any of the designed combinations of MD, PSF, and BA, suggesting efficient utilization of these wastes in the unfired admixed soil blocks.
(f) XRD and XRF characterization of the marble dust and bagasse ash supports the results showing that improvements in the strength attributes of unfired admixed soil blocks are due to the presence of significant contents of lime and silica.
(g) The microstructural analysis of the samples performed via SEM and EDS showed improved bonding with PSF and PSF–binders–soil mixture.
(h) These outcomes show that the recommended technique is exceptionally effective at enhancing the physical characteristics of unfired admixed soil blocks, and represents an economical and environmentally friendly solution.

5. Scope of Future Work

The impact of marble dust, paddy straw fiber, and bagasse ash on other properties of unfired admixed soil blocks, such as their thermal conductivity, porosity, permeability, etc., can be estimated.

Further research can be carried out on the impact of other types of natural and artificial fibers on the properties of soil blocks admixed with marble dust and bagasse ash. Such materials include coir, banana fiber, plastic fibers extruded from plastic bags, disposable plastic products, etc. This could greatly boost the usage of plastic trash and natural waste fibers in the building sector.

Further research can be carried out on the impact of other types of binders on the properties of unfired admixed soil blocks reinforced with PSF.

Author Contributions: Conceptualization, T.S., S.S. (Sandeep Singh), S.S. (Shubham Sharma), A.S. and A.K.S.; methodology, T.S., S.S. (Sandeep Singh), S.S. (Shubham Sharma), A.S. and A.K.S.; formal analysis, T.S., S.S. (Sandeep Singh), S.S. (Shubham Sharma), A.S. and A.K.S.; investigation, T.S., S.S. (Sandeep Singh), S.S. (Shubham Sharma), A.S. and A.K.S.; writing—original draft preparation, T.S., S.S. (Sandeep Singh), S.S. (Shubham Sharma), A.S. and A.K.S.; writing—review and editing, S.S. (Shubham Sharma), C.L., Y.Z. and E.M.T.E.; supervision, S.S. (Shubham Sharma), C.L., Y.Z. and E.M.T.E.; project administration, S.S. (Shubham Sharma) and E.M.T.E.; funding acquisition, S.S. (Shubham Sharma) and E.M.T.E. All authors have read and agreed to the published version of the manuscript.

Funding: This research received no external funding.

Institutional Review Board Statement: Not applicable.

Informed Consent Statement: Not applicable.

Data Availability Statement: No data were used to support this study.

Acknowledgments: The authors would like to acknowledge the support of Future University in Egypt for paying the Article Processing Charges (APC) of this publication.

Conflicts of Interest: The authors declare no conflict of interest.

Abbreviations

PSF	paddy straw fibre
MD	marble dust
BA	bagasse ash
STS	split tensile strength
SEM	Scanning Electron Microscope
EDS	Energy Dispersive X-ray Spectroscopy

References

1. Lejano, B.A.; Gabaldon, R.J.; Go, P.J.; Juan, C.G.; Wong, M. Compressed earth blocks with powdered green mussel shell as partial binder and pig hair as fiber reinforcement. *Int. J. Geomate* **2019**, *16*, 137–143. [CrossRef]
2. James, J.; Saraswathy, R. Performance of Fly Ash-Lime Stabilized Lateritic Soil Blocks Subjected to Alternate Cycles of Wetting and Drying. *Civ. Environ. Eng.* **2020**, *16*, 30–38. [CrossRef]
3. Sharma, T.; Singh, S.; Singh Thind, P.; Singh Chohan, J.; Kumar, R.; Sharma, S.; Kaplonek, W.; Khalilpoor, N.; Issakhov, A. A Systematic Review on the Performance Characteristics of Sustainable, Unfired Admixed Soil Blocks for Agricultural and Industrial Waste Management. *Adv. Mater. Sci. Eng.* **2021**, *2021*, 1749694. [CrossRef]
4. Carvalho, A.; de Castro Xavier, G.; Alexandre, J.; Pedroti, L.G.; de Azevedo, A.R.G.; Vieira, C.M.F.; Monteiro, S.N. Environmental durability of soil-cement block incorporated with ornamental stone waste. *Mater. Sci. Forum* **2014**, *798–799*, 548–553. [CrossRef]
5. Jittabut, P. Physical properties and thermal conductivity of soil geopolymer block. *J. Phys. Conf. Ser.* **2019**, *1380*, 012038. [CrossRef]
6. Danso, H.; Martinson, D.B.; Ali, M.; Williams, J.B. Mechanisms by which the inclusion of natural fibres enhance the properties of soil blocks for construction. *J. Compos. Mater.* **2017**, *51*, 3835–3845. [CrossRef]
7. Danso, H.; Martinson, D.B.; Ali, M.; Williams, J.B. Physical, mechanical and durability properties of soil building blocks reinforced with natural fibres. *Constr. Build. Mater.* **2015**, *101*, 797–809. [CrossRef]
8. Danso, H.; Martinson, D.B.; Ali, M.; Williams, J. Effect of fibre aspect ratio on mechanical properties of soil building blocks. *Constr. Build. Mater.* **2015**, *83*, 314–319. [CrossRef]
9. Alexandre, J.; de Assis Paula e Silva, C.L.; de Azevedo, A.R.G.; de Castro Xavier, G.; Candido, V.S.; Monteiro, S.N. Processing and properties of soil-cement blocks incorporated with natural grit. *Mater. Sci. Forum* **2014**, *798–799*, 343–346. [CrossRef]
10. Kwan, W.H.; Cheah, C.B.; Ramli, M.; Al-Sakkaf, Y.K. Incorporation of bitumen and calcium silicate in cement and lime stabilized soil blocks. *AIP Conf. Proc.* **2017**, *1828*, 20011. [CrossRef]

11. França, B.R.; Azevedo, A.R.G.; Monteiro, S.N.; Da Costa, F.; Filho, G.; Marvila, M.T.; Alexandre, J.; Zanelato, E.B. Durability of soil-Cement blocks with the incorporation of limestone residues from the processing of marble. *Mater. Res.* **2018**, *21*, e20171118. [CrossRef]
12. Figueiredo, S.S.; Silva, C.G.; Bezerra, I.M.T.; Dias, S.L.; Neves, G.A.; Menezes, R.R.; de Lima Santana, L.N. Soil-lime blocks using construction residues—Durability study. *Mater. Sci. Forum* **2012**, *727–728*, 1422–1427. [CrossRef]
13. Yoosathaporn, S.; Pathom-aree, W.; Tiangburanatham, P. The influence of biocalcification on soil-cement interlocking block compressive strength. *Biotechnol. Agron. Soc. Environ.* **2015**, *19*, 262–269.
14. Sujatha, E.R.; Selsia Devi, S. Reinforced soil blocks: Viable option for low cost building units. *Constr. Build. Mater.* **2018**, *189*, 1124–1133. [CrossRef]
15. Sharma, T.; Singh, S. Characteristics of unfired soil blocks stabilized with industrial waste and agricultural waste. *IOP Conf. Ser. Earth Environ. Sci.* **2021**, *889*, 12041. [CrossRef]
16. Alavéz-Ramírez, R.; Montes-García, P.; Martínez-Reyes, J.; Altamirano-Juárez, D.C.; Gochi-Ponce, Y. The use of sugarcane bagasse ash and lime to improve the durability and mechanical properties of compacted soil blocks. *Constr. Build. Mater.* **2012**, *34*, 296–305. [CrossRef]
17. Salim, R.W.; Ndambuki, J.M.; Adedokun, D.A. Improving the bearing strength of sandy loam soil compressed earth block bricks using Sugercane Bagasse Ash. *Sustainability* **2014**, *6*, 3686–3696. [CrossRef]
18. *BIS:2720 (Part 1)*; Indian Standard Methods of Test for Soils: Preparation of Dry Soil Samples for Various Tests. Bureau of Indian Standards: New Delhi, India, 2006.
19. *BIS.IS 3495 (Parts 1–4)*; IS 3495: 1992—Parts 1 to 4—Methods of Tests of Burnt Clay Building Bricks. Bureau of Indian Standards: New Delhi, India, 1992.
20. Donkor, P.; Obonyo, E. Compressed soil blocks: Influence of fibers on flexural properties and failure mechanism. *Constr. Build. Mater.* **2016**, *121*, 25–33. [CrossRef]
21. Tomar, A.; Sharma, T.; Singh, S. Strength properties and durability of clay soil treated with mixture of nano silica and Polypropylene fiber. *Mater. Today Proc.* **2020**, *26*, 3449–3457. [CrossRef]
22. Meng, Y.; Yan, T.; Muhammad, Y.; Li, J.; Qin, P.; Ling, L.; Rong, H.; Yang, X. Study on the performance and sustainability of modified waste crumb rubber and steel slag powder/SBS composite modified asphalt mastic. *J. Clean. Prod.* **2022**, *338*, 130563. [CrossRef]
23. Munshi, S.; Sharma, R.P. Utilization of rice straw ash as a mineral admixture in construction work. *Mater. Today Proc.* **2019**, *11*, 637–644. [CrossRef]
24. Xu, J.; Lan, W.; Ren, C.; Zhou, X.; Wang, S.; Yuan, J. Modeling of coupled transfer of water, heat and solute in saline loess considering sodium sulfate crystallization. *Cold Reg. Sci. Technol.* **2021**, *189*, 103335. [CrossRef]
25. Xu, J.; Zhou, L.; Hu, K.; Li, Y.; Zhou, X.; Wang, S. Influence of Wet-Dry Cycles on Uniaxial Compression Behavior of Fissured Loess Disturbed by Vibratory Loads. *KSCE J. Civ. Eng.* **2022**, *26*, 2139–2152. [CrossRef]
26. Wu, Z.; Xu, J.; Chen, H.; Shao, L. Shear Strength and Mesoscopic Characteristics of Basalt Fiber–Reinforced Loess after Dry–Wet Cycles. *J. Mater. Civ. Eng.* **2022**, *34*. [CrossRef]
27. Yuan, J.; Lei, D.; Shan, Y.; Tong, H.; Fang, X.; Zhao, J. Direct Shear Creep Characteristics of Sand Treated with Microbial-Induced Calcite Precipitation. *Int. J. Civ. Eng.* **2022**, *20*, 763–777. [CrossRef]
28. Shan, Y.; Zhao, J.; Tong, H.; Yuan, J.; Lei, D.; Li, Y. Effects of activated carbon on liquefaction resistance of calcareous sand treated with microbially induced calcium carbonate precipitation. *Soil Dyn. Earthq. Eng.* **2022**, *161*, 107419. [CrossRef]
29. Hu, Z.; Shi, T.; Cen, M.; Wang, J.; Zhao, X.; Zeng, C.; Zhou, Y.; Fan, Y.; Liu, Y.; Zhao, Z. Research progress on lunar and Martian concrete. *Constr. Build. Mater.* **2022**, *343*, 128117. [CrossRef]
30. Liu, E.; Chen, S.; Yan, D.; Deng, Y.; Wang, H.; Jing, Z.; Pan, S. Detrital zircon geochronology and heavy mineral composition constraints on provenance evolution in the western Pearl River Mouth basin, northern south China sea: A source to sink approach. *Mar. Pet. Geol.* **2022**, *145*, 105884. [CrossRef]
31. Zhu, Z.; Zhu, Z.; Wu, Y.; Han, J. A Prediction Method of Coal Burst Based on Analytic Hierarchy Process and Fuzzy Comprehensive Evaluation. *Front. Earth Sci.* **2022**, *9*, 1424. [CrossRef]
32. Bai, B.; Zhou, R.; Cai, G.; Hu, W.; Yang, G. Coupled thermo-hydro-mechanical mechanism in view of the soil particle rearrangement of granular thermodynamics. *Comput. Geotech.* **2021**, *137*, 104272. [CrossRef]
33. Zhang, Z.; Yang, F.; Zhang, H.; Zhang, T.; Wang, H.; Xu, Y.; Ma, Q. Influence of CeO_2 addition on forming quality and microstructure of TiCx-reinforced CrTi4-based laser cladding composite coating. *Mater. Charact.* **2020**, *171*, 110732. [CrossRef]
34. Wang, Z.; Qiang, H. Mechanical properties of thermal aged HTPB composite solid propellant under confining pressure. *Def. Technol.* **2021**, *18*, 618–625. [CrossRef]
35. Wang, Z.; Qiang, H.; Wang, J.; Duan, L. Experimental Investigation on Fracture Properties of HTPB Propellant with Circumferentially Notched Cylinder Sample. *Propellants Explos. Pyrotech.* **2022**, *47*, e202200046. [CrossRef]
36. Cheng, H.; Sun, L.; Wang, Y.; Chen, X. Effects of actual loading waveforms on the fatigue behaviours of asphalt mixtures. *Int. J. Fatigue* **2021**, *151*, 106386. [CrossRef]
37. Xu, H.; Wang, X.; Liu, C.; Chen, J.; Zhang, C. A 3D root system morphological and mechanical model based on L-Systems and its application to estimate the shear strength of root-soil composites. *Soil Tillage Res.* **2021**, *212*, 105074. [CrossRef]

38. Shi, L.; Xiao, X.; Wang, X.; Liang, H.; Wang, D. Mesostructural characteristics and evaluation of asphalt mixture contact chain complex networks. *Constr. Build. Mater.* **2022**, *340*, 127753. [CrossRef]
39. Lan, M.Y.; Zheng, B.; Shi, T.; Ma, C.; Liu, Y.; Zhao, Z. Crack resistance property of carbon nanotubes-modified concrete. *Mag. Concr. Res.* **2022**, *8*, 29–37. [CrossRef]
40. Gu, M.; Mo, H.; Qiu, J.; Yuan, J.; Xia, Q. Behavior of Floating Stone Columns Reinforced with Geogrid Encasement in Model Tests. *Front. Mater.* **2022**, *9*, 503. [CrossRef]
41. Safaei, B.; Davodian, E.; Fattahi, A.M.; Asmael, M. Calcium Carbonate Nanoparticles Effects on Cement Plast Properties. *Microsyst. Technol.* **2021**, *27*, 3059–3076.